Satellite-derived direct radiative effect of aerosols dependent on cloud cover

D. Chand[1]*, R. Wood[1], T. L. Anderson[1], S. K. Satheesh[2,3] and R. J. Charlson[1]

Aerosols from biomass burning can alter the radiative balance of the Earth by reflecting and absorbing solar radiation[1]. Whether aerosols exert a net cooling or a net warming effect will depend on the aerosol type and the albedo of the underlying surface[2]. Here, we use a satellite-based approach to quantify the direct, top-of-atmosphere radiative effect of aerosol layers advected over the partly cloudy boundary layer of the southeastern Atlantic Ocean during July–October of 2006 and 2007. We show that the warming effect of aerosols increases with underlying cloud coverage. This relationship is nearly linear, making it possible to define a critical cloud fraction at which the aerosols switch from exerting a net cooling to a net warming effect. For this region and time period, the critical cloud fraction is about 0.4, and is strongly sensitive to the amount of solar radiation the aerosols absorb and the albedo of the underlying clouds. We estimate that the regional-mean warming effect of aerosols is three times higher when large-scale spatial covariation between cloud cover and aerosols is taken into account. These results demonstrate the importance of cloud prediction for the accurate quantification of aerosol direct effects.

Aerosols derived from biomass burning make a significant but poorly quantified contribution to anthropogenic radiative forcing of climate[1–3] and may affect regional atmospheric circulation[4]. The most significant differences between model estimates of the top-of-atmosphere direct climate forcing (DCF) are in regions where these aerosols dominate the forcing[3]. DCF is the change in the top-of-atmosphere direct radiative effect (DRE_{toa}) since pre-industrial times and cannot be determined from modern measurements alone[5]. Both DRE_{toa} and the absorption within the atmosphere (DRE_{atm}) are sensitive to aerosol optical properties (chiefly aerosol optical thickness τ, absorption and size distribution)[6], and also to the albedo of the underlying surface[7,8]. In the absence of clouds, DRE_{toa} is negative over the ocean owing to its low surface albedo even when the aerosol is strongly absorbing[9]. However, when absorbing aerosol layers are located above clouds, DRE_{toa} can be positive[2,10]. Although a few modelling studies have attempted to quantify the regional effects of clouds on the DRE (for example, ref. 10), here we use spaceborne lidar observations of aerosols above clouds, together with observed cloud optical properties, to quantify the aerosol DRE and the effect of clouds on it.

Previous intensive observational studies of aerosols derived from biomass burning, conducted during field campaigns over North and South America[11–13] and Africa[14,15], are limited either in time or space. Passive remote sensing of aerosol optical properties is routinely conducted at numerous surface sites across the globe (for example, the AERONET project[16]) and from satellites[17–19],

but such approaches fail or are highly biased in the presence of clouds[18,20], which severely limits our ability to quantify the radiative effects of aerosols in regions where aerosols are advected over low-level clouds.

Here, we quantify the optical depth τ and ångström exponent å of aerosol layers overlying optically thick clouds over the southern Atlantic Ocean using spaceborne lidar observations from Cloud Aerosol Lidar and Infrared Pathfinder Satellite Observation (CALIPSO), using the retrieval method of Chand *et al.*[21]. An elevated layer is here defined as being a layer with a detectable optical thickness overlying a strongly attenuating cloud that has a top below 3 km, although over much of the domain the low-cloud top height is significantly lower than this (see Supplementary Fig. S1 on the heights of the cloud and elevated aerosol layers). For the elevated aerosol layers, we use the CALIPSO layer identification algorithm[21] to determine the aerosol-layer top and base height. Most elevated aerosol-layer top heights fall between 2.5–5.5 km and have a mean thickness of approximately 2 km. Most of the clouds (86%) are observed below 3 km over the entire domain. The mode of the cloud base and top of these low-level clouds are about 0.7 km and 1.3 km, respectively. If the uppermost cloud layer is above 3 km, the aerosol optical thickness is assumed to be zero for the purposes of the radiative transfer calculations. Other data-selection details are given in the Methods section and in Chand *et al.*[21].

Figure 1 shows an example of the vertical and along-track structure of clouds and elevated aerosol layers during a night-time CALIPSO pass in August 2006. Our aerosol retrieval algorithm indicates that the τ of the elevated aerosol layers is in places as high as 1.5. The lower detection limit of the τ retrieval is estimated to be 0.07. Data from each month (July–October) for the years 2006 and 2007 are integrated to obtain a seasonal average over the Atlantic Ocean (7.5° N–22.5° S, 17.5° E–27.5° W).

We use the DISORT radiative transfer model (RTM; see the Methods section) to estimate the DRE of elevated aerosol layers overlying clouds and for clear-sky conditions over land and ocean. The model inputs are the optical properties (τ, single scattering albedo ϖ, å and asymmetry factor g) and geometrical properties (height and thickness) of the elevated aerosol layer and the albedo of the surface underlying the aerosol layer (either the cloud or surface albedo).

For the RTM, we use τ and å from CALIPSO using a newly developed, above-cloud retrieval (see the Methods section and ref. 21). τ is retrieved at 532 nm and å applies to the wavelength dependence of τ between 532 and 1,064 nm. The model results depend quite strongly on ϖ, which cannot currently be determined from spaceborne observations[22]. Here, we use ϖ (at 550 nm) = 0.85 ± 0.02 (regional mean and uncertainty)

[1]Department of Atmospheric Science, University of Washington, Box 351640, Seattle, Washington, USA, [2]Centre for Atmospheric and Oceanic Sciences, Indian Institute of Science, Bangalore-560 012, India, [3]NASA Goddard Space Flight Center, Greenbelt, Maryland 20771, USA. *e-mail: duli@atmos.washington.edu.
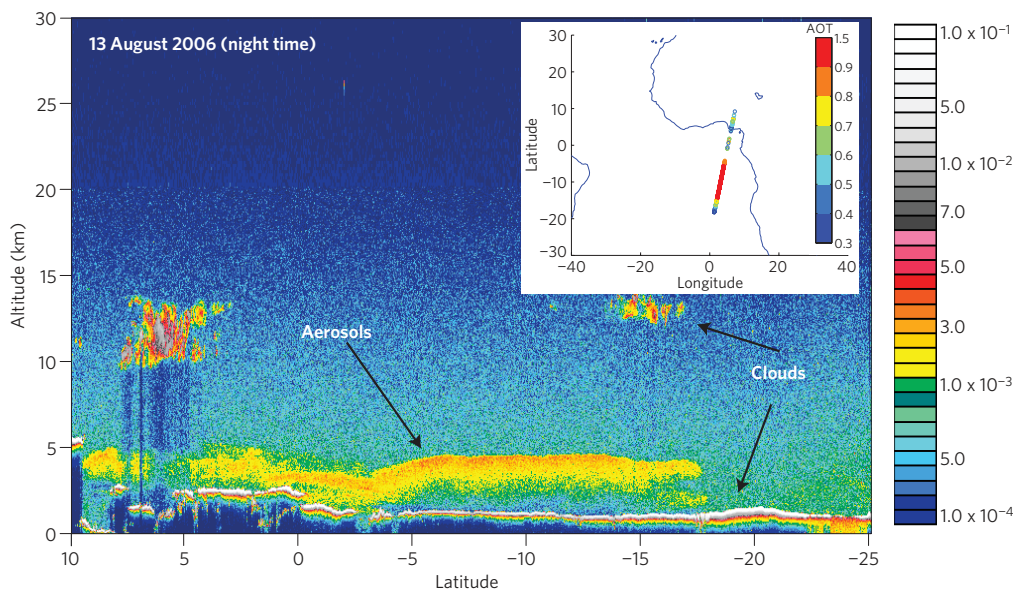
Figure 1 | Profiles of 532 nm backscatter return signal from the CALIPSO lidar showing the vertical distribution of aerosols and underlying clouds. Aerosol optical thickness (AOT) is shown in the inset. Strong backscattering ($>0.001\,\mathrm{sr}^{-1}\,\mathrm{km}^{-1}$) is associated with aerosol and/or cloud layers (as indicated by arrows). Observations from 2006 and 2007 indicate that such events are very frequent during the biomass-burning season (particularly August and September) over the west coast of Africa between the Equator and 20° S.

on the basis of an updated synthesis of remote and *in situ* measurements during the Southern African Regional Science Initiative 2000 (ref. 23). For reasons discussed elsewhere[23], we consider this range of values more reliable than the value of 0.91 ± 0.04 derived by Haywood *et al.*[24] during this same campaign. We set $g = 0.62 \pm 0.03$ (550 nm), consistent with size distributions of laboratory-generated and field-observed biomass-burning aerosols over Southern Africa[24] and South America (Chand *et al.*, unpublished data and ref. 25).

The regional distribution of mean τ (Fig. 2a) clearly indicates that elevated aerosol layers of significant optical thickness are present over the southern Atlantic at distances of over 2,000 km from the South African coast, consistent with advection by the mean flow from the continental biomass-burning sources[14,26]. Much of the advection seems to be in a zonal direction consistent with the predominantly easterly winds at 600 hPa north of 15° S. Weak meridional advection confines most of the aerosols to south of the intertropical convergence zone. The derived diurnal and seasonal (July–October) mean values of DRE demonstrate a major impact of elevated aerosols on the radiative budget of the atmosphere ($\mathrm{DRE_{atm}}$, Fig. 2b) and the climate system ($\mathrm{DRE_{toa}}$, Fig. 2c). Note that $\mathrm{DRE_{toa}}$ changes sign reflecting the geographic variability in the underlying cloud fractional coverage C. This moves the region of strongest positive $\mathrm{DRE_{toa}}$ some 5° south from the region with maximum τ towards the region with maximum C. Conversely, the $\mathrm{DRE_{toa}}$ just south of the Equator over the ocean is reduced because the cloud fraction there is much lower. These results clearly show that the pattern of cloud cover variability beneath the aerosol layers has a first-order impact on the regional distribution of aerosol radiative forcing.

The impact of the underlying cloud is more clearly demonstrated by examination of the radiative forcing efficiency ($\mathrm{RFE_{toa}} = \mathrm{DRE_{toa}}/\tau$) of the elevated aerosol layers (Fig. 3). There is a remarkably strong correlation between $\mathrm{RFE_{toa}}$ and the monthly mean value of C ($r^2 = 0.96$), implying that the cloud fractional coverage is an excellent predictor of the mean $\mathrm{RFE_{toa}}$ in a particular region on a monthly timescale. $\mathrm{RFE_{toa}}$ for clear-sky conditions is inferred to be $-34\,\mathrm{W\,m^{-2}}\,\tau^{-1}$, whereas the mean value for cloudy sky is $52\,\mathrm{W\,m^{-2}}\,\tau^{-1}$, indicating an average increase in $\mathrm{RFE_{toa}}$ of

$0.86\,\mathrm{W\,m^{-2}}$ per unit τ for 1% increase in cloud cover. The critical cloud fraction C_{crit}, for which $\mathrm{DRE_{toa}}$ changes sign, is 0.40. On the basis of the Terra data used herein, the average cloud coverage over this region is 0.48, leading to a positive estimate for $\mathrm{DRE_{toa}}$ ($2.4\,\mathrm{W\,m^{-2}}$) for the region as a whole. Importantly, this is three times as large as that ($0.8\,\mathrm{W\,m^{-2}}$) obtained by assuming that the spatial pattern of τ (of which the seasonal-regional mean value is 0.11) is independent of C, emphasizing the importance not only of the mean cloud fractional coverage but also its spatial distribution with respect to the overlying aerosol layers. There is a tendency for regions with optically thick aerosol layers to be those with a fractional coverage of low clouds exceeding that for the domain as a whole. Thus, knowledge of the domain mean cloud cover and mean aerosol optical thickness is insufficient to determine the regional mean DRE, and the covariance between the two must be considered. This is a stringent challenge for global climate models, which exhibit considerable deficiencies in their ability to represent the correct optical properties of both clouds[27] and aerosols[3].

The value of C_{crit} derived herein (0.40) is sensitive to uncertainties in aerosol optical properties (see Supplementary Fig. S3). Increasing ϖ over its uncertainty range of 0.83–0.87 leads to an increase of almost 0.1 in C_{crit} (from 0.37 to 0.47). This constitutes the greatest source of explicitly estimated error in our study. Changing å and g over their uncertainty ranges (1.1–2.1 and 0.59–0.65, respectively) causes C_{crit} to vary by 0.04 in each case. In contrast, shifting cloud altitude by 1.25 km had only a minor effect on C_{crit} of 0.01.

Podgorny and Ramanathan used an RTM to estimate the top-of-atmosphere radiative effect of absorbing aerosols over broken low clouds in the Indian Ocean[10]. Assuming thick clouds and moderately absorbing aerosol ($\varpi = 0.90$ at 500 nm), they found a similar strong dependence on cloud fraction, but a lower value of C_{crit} (0.25) than found herein (0.40). Adjusting for the difference in ϖ would increase this discrepancy. The explanation for this difference seems to be cloud albedo, which is calculated from cloud optical depth within the RTMs of both studies. In our study, cloud albedos are 0.50 ± 0.06 (Jul.–Oct. 5° × 5° mean and standard deviation) on the basis of Moderate Resolution Imaging Spectroradiometer (MODIS)-retrieved cloud optical depths of
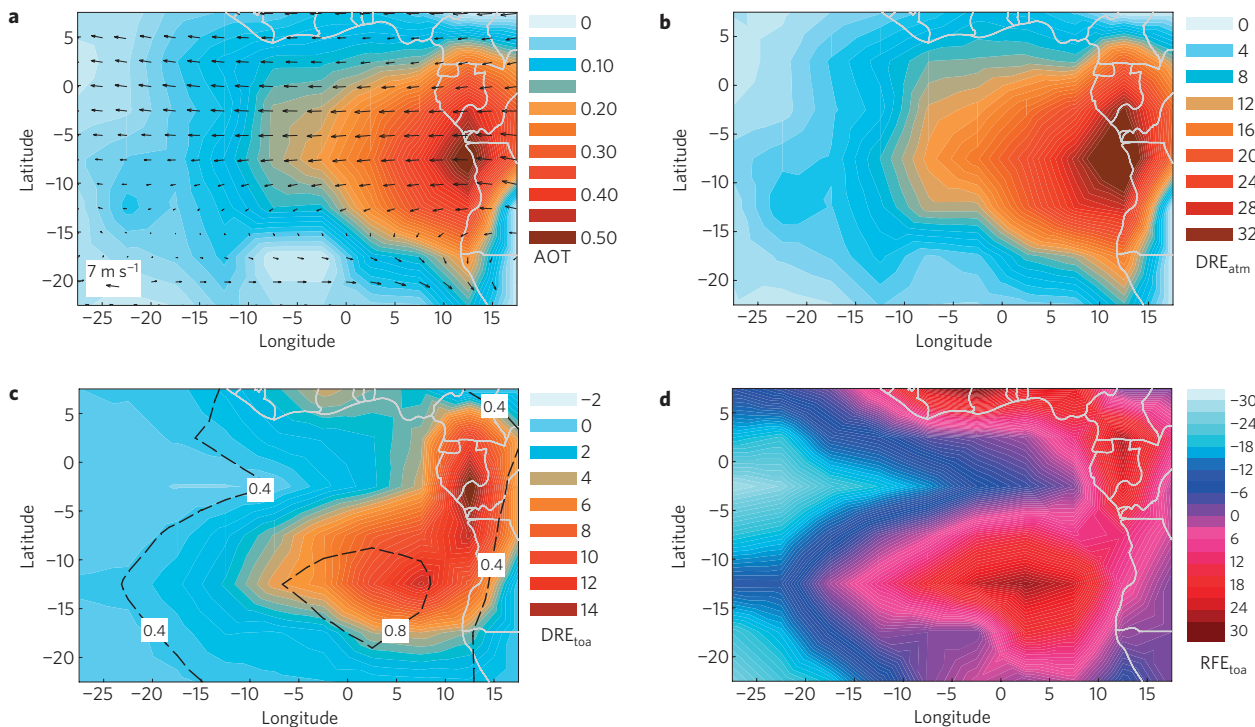
Figure 2 | Regional distributions of aerosols, aerosol radiative impacts, winds and cloud fraction. a–d, Maps showing seasonal (July–October 2006/2007) mean values of aerosol optical thickness τ (including zeros when no elevated aerosol layer is detected) and National Centers for Environmental Prediction winds at 600 hPa (**a**), DRE_{atm} (column absorption) (**b**), DRE_{toa} (DRE_{toa} shown by colours and cloud fraction shown by contour lines) (**c**) and the direct RFE ($RFE = DRE_{toa}/\tau$) (**d**). The τ and cloud fraction are retrieved from CALIPSO satellite and MODIS Terra satellite, respectively.
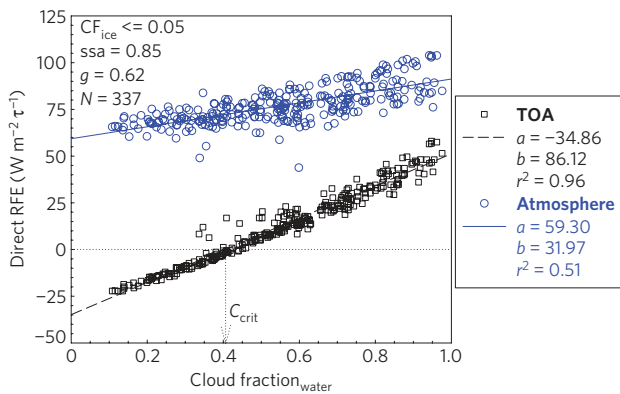

Figure 3 | Correlation of aerosol direct RFE with cloud fraction for July–October 2006–2007. RFE at the top of the atmosphere (squares) and within the atmosphere (circles) as a function of cloud fraction. C_{crit} is the cloud fraction when the top-of-atmosphere (TOA) RFE changes sign.

7.8 ± 1.8. The calculations by Podgorny and Ramanathan assumed a cloud optical depth of 15, implying much higher cloud albedo (close to 0.7). This would cause aerosol over cloud to have a much stronger warming effect, lowering the balance point, C_{crit}. We see from this comparison that accurate knowledge of cloud albedo (in addition to C, τ and ϖ) is critical to the accurate determination of aerosol radiative forcing.

Small-scale or day-to-day covariation among aerosol and underlying cloud properties (assumed herein to be zero; see the Methods section) constitutes an extra, unknown source of error in our estimates. A recent study conducted in the same region of the southeast Atlantic[28] demonstrates covariation of τ and C at scales smaller than the 5° averaging used herein. However, this finding relied on retrieving both

quantities from MODIS, and the authors were careful to point out that the cause could be either a physical relationship or an instrumental artefact. If physical, such covariation would tend to increase the warming effect of the aerosol and lower C_{crit}. Covariations among other combinations of key properties (C, cloud albedo, τ and ϖ) could also be important and should be investigated in future studies.

A recent comparison of global models showed that the southeast Atlantic region exhibits extremely large inter-model differences in all-sky direct radiative forcing[3]. Even in the annual mean, the modelled values of radiative forcing over this region vary from -1 to $+2\,W\,m^{-2}$. These estimates are poorly constrained by traditional aerosol retrievals from passive remote sensing because these methods are restricted to clear-sky situations. As shown herein, above-cloud aerosol retrievals from CALIPSO, combined with cloud retrievals from passive satellites, provide a powerful new set of tools for adjudicating among the discordant model estimates and, ultimately, improving understanding of aerosol radiative forcing and its dependence on underlying clouds.

Methods

On the basis of the active remote sensing observations from the 532 and 1,064 nm channels on CALIPSO, we developed a new method to quantify the aerosol optical depth (τ) and ångström exponent (å) of aerosol layers above clouds[21]. Here, we applied this technique regionally over the southern Atlantic Ocean (7.5° N–22.5° S, 17.5° E–27.5° W) to produce monthly mean τ and å estimates at 5° × 5° resolution for two biomass-burning seasons (July–October of 2006 and 2007). Data from the MODIS on the NASA Terra satellite are used to provide monthly mean estimates (also at 5° × 5° resolution) of ice-cloud fractional coverage (used as a data selection screen), water-cloud fractional coverage C and water-cloud visible albedo, where the last of these derives from water-cloud optical thickness retrievals[29] and two-stream radiative transfer theory[30]. Cloud data from MODIS provide essentially complete coverage of each 5° × 5° block every day; however, the daily, spatial coverage by CALIPSO is much lower. For this reason, we use both daytime and night-time CALIPSO data and we aggregate them to monthly averages before combining them with MODIS data to calculate direct radiative forcing. Thus, our method assumes (1) that above-cloud aerosol in this region

does not exhibit significant diurnal variation, (2) that the above-cloud aerosols detected by CALIPSO along its orbit are representative of the entire 5° × 5° block and (3) that there is no day-to-day covariation of cloud fraction or properties with above-cloud aerosol properties. We have tested (1) and found an root mean square difference of day versus night τ of 12%, which would bias the average of the two by no more than 6%. This is well within the uncertainties of our retrieval method. Assumptions (2) and (3) seem to be reasonable, but should be tested in follow-up studies.

The direct RFE of elevated aerosol layers is calculated using the DISORT radiative transfer code[31]. Calculations are carried out for each 5° × 5° block at monthly-mean resolution. Because we do not explicitly model the effects of cirrus clouds, blocks where ice-cloud fraction is greater than 5% were excluded from the results shown in Fig. 3. This excludes about 40% of the available blocks. Calculations run without this screening are noisier (for example, the correlation between RFE and C is somewhat lower than indicated in Fig. 3; see Supplementary Fig. S4) but yield almost identical values of domain-mean DRE and C_{crit}. We carry out separate calculations for aerosols in a clear-sky situation (assuming an ocean surface albedo of 0.06 and a land surface albedo 0.25) and above a cloudy surface having the observationally determined mean albedo. We apply the mean cloud and aerosol heights observed by CALIPSO over the entire domain. We carry out extra calculations to determine the sensitivity of domain-mean DRE and C_{crit} to the fixed values of ϖ, g, å, cloud height and aerosol height (see Supplementary Figs S1–S4). These calculations indicate that DRE and C_{crit} are most sensitive to ϖ followed by g and å. As long as the aerosol layer is separated from the cloud layer by at least a few hundred meters, changes in cloud or aerosol height have negligible effects.

References

1. Intergovernmental Panel of Climate Change (IPCC). *The Physical Science Basis, Contribution of Working Group I to the Fourth Assessment Report of the IPCC* 916 (Cambridge Univ. Press, 2007).
2. Keil, A. & Haywood, J. M. Solar radiative forcing by biomass burning aerosol particles during SAFARI 2000: A case study based on measured aerosol and cloud properties. *J. Geophys. Res.* **108**, 8467 (2003).
3. Schulz, M. *et al.* Radiative forcing by aerosols as derived from the AeroCom present-day and pre-industrial simulations. *Atmos. Chem. Phys.* **6**, 5225–5246 (2006).
4. Ramanathan, V. & Carmichael, G. Global and regional climate changes due to black carbon. *Nature Geosci.* **1**, 221–227 (2008).
5. Bellouin, N., Jones, A., Haywood, J. & Christopher, S. A. Updated estimate of aerosol direct radiative forcing from satellite observations and comparison against the Hadley Centre climate model. *J. Geophys. Res.* **113**, D10205 (2008).
6. Haywood, J. & Boucher, O. Estimates of the direct and indirect radiative forcing due to tropospheric aerosols: A review. *Rev. Geophys.* **38**, 513–543 (2000).
7. Chýlek, P. & Coakley, J. A. Jr. Aerosol and climate. *Science* **183**, 75–77 (1974).
8. Seinfeld, J. Black carbon and brown clouds. *Nature Geosci.* **1**, 15–16 (2008).
9. Satheesh, S. K. & Ramanathan, V. Large differences in tropical aerosol forcing at the top of the atmosphere and Earth's surface. *Nature* **405**, 60–63 (2000).
10. Podgorny, I. A. & Ramanathan, V. A modeling study of the direct effect of aerosols over the tropical Indian Ocean. *J. Geophys. Res.* **106**, 24097–24105 (2001).
11. Fishman, J., Hoell, J. M., Bendura, R. D., McNeal, R. J. & Kirchhoff, V. W. J. H. NASA GTE TRACE-A experiment (September–October, 1992). *J. Geophys. Res.* **101**, 23865–23879 (1996).
12. Kaufman, Y. J. *et al.* Smoke, clouds and radiation-Brazil (SCAR-B) experiment. *J. Geophys. Res.* **103**, 31783–31808 (1998).
13. Andreae, M. O. *et al.* Biomass-burning emissions and associated haze layers over Amazonia. *J. Geophys. Res.* **93**, 1509–1527 (1988).
14. Andreae, M. O. *et al.* Influence of plumes from biomass burning on atmospheric chemistry over the equatorial Atlantic during CITE-3. *J. Geophys. Res.* **99**, 12793–12808 (1994).
15. Lindesay, J. A. *et al.* International geosphere biosphere programme/international global atmospheric chemistry SAFARI-92 field experiment: Background and overview. *J. Geophys. Res.* **101**, 23521–23530 (1996).
16. Holben, B. N. *et al.* AERONET: A federated instrument network and data archive for aerosol characterization. *Remote Sens. Environ.* **66**, 1–16 (1998).
17. King, M. D., Kaufman, Y. J., Menzel, W. P. & Tanre, D. Remote sensing of cloud, aerosol, and water vapor properties from the moderate resolution imaging spectrometer (MODIS). *IEEE Trans. Geosci. Remote Sens.* **30**, 2–27 (1992).
18. Remer, L. A. *et al.* The MODIS aerosol algorithm, products, and validation. *J. Atmos. Sci.* **62**, 947–973 (2005).
19. Myhre, L. *et al.* Regional aerosol optical properties and radiative impact of the extreme smoke event in the European Arctic in spring 2006. *Atmos. Chem. Phys.* **7**, 5899–5915 (2007).
20. Kaufman, Y. J., Remer, L. A. & Tanre, D. A critical examination of the residual cloud contamination and diurnal sampling effects on MODIS estimates of aerosol over ocean. *IEEE Trans. Geosci. Remote Sens.* **43**, 2886–2897 (2005).
21. Chand, D. *et al.* Quantifying above-cloud aerosol using spaceborne lidar for improved understanding of cloudy-sky direct climate forcing. *J. Geophys. Res.* **113**, D13206 (2008).
22. Mishchenko, M. I. *et al.* Accurate monitoring of terrestrial aerosols and total solar irradiance: Introducing the glory mission. *Bull. Am. Meteorol. Soc.* **88**, 677–691 (2007).
23. Leahy, L. V., Anderson, T. L., Eck, T. F. & Bergstrom, R. W. A synthesis of single scattering albedo of biomass burning aerosol over southern Africa during SAFARI 2000. *Geophys. Res. Lett.* **34**, L12814 (2007).
24. Haywood, J. M. *et al.* The mean physical and optical properties of regional haze dominated by biomass burning aerosol measured from the C-130 aircraft during SAFARI 2000. *J. Geophys. Res.* **108**, 8473 (2003).
25. Chand, D. *et al.* Optical and physical properties of aerosols in the boundary layer and free troposphere over the Amazon Basin during the biomass burning season. *Atmos. Chem. Phys.* **6**, 2911–2925 (2006).
26. Anderson, T. L. *et al.* An 'A-Train' strategy for quantifying direct climate forcing by anthropogenic aerosols. *Bull. Am. Meteorol. Soc.* **86**, 1795–1809 (2005).
27. Karlsson, J., Svensson, G. & Rodhe, H. Cloud radiative forcing of subtropical low level clouds in global models. *Clim. Dyn.* **30**, 779–788 (2008).
28. Loeb, N. G. & Schuster, G. L. An observational study of the relationship between cloud, aerosol and meteorology in broken low-level cloud conditions. *J. Geophys. Res.* **113**, doi:10.1029/2007JD009763 (2008).
29. King, M. D., Tsay, S. C., Platnick, S. E., Wang, M. & Liou, K. N. *Cloud Retrieval Algorithms for MODIS: Optical Thickness, Effective Particle Radius, and Thermodynamic Phase.* MODIS Algorithm Theoretical Basis Doc. ATBD-MOD-05 (NASA, 1997).
30. Coakley, J. A. & Chýlek, P. The two-stream approximation in radiative transfer: Including the angle of the incident radiation. *J. Atmos. Sci.* **32**, 409 (1975).
31. Ricchiazzi, P., Yang, S., Gautier, C. & Sowle, D. SBDART: A research and teaching tool for plane-parallel radiative transfer in the Earth's atmosphere. *Bull. Am. Meteorol. Soc.* **79**, 2101–2114 (1998).

Author contributions

D.C. carried out the bulk of the analysis of CALIPSO data using a retrieval algorithm designed by D.C., T.L.A., R.W. and R.J.C. (plus colleagues at NASA Langley). MODIS cloud data were synthesized by R.W., D.C. and S.K.S. carried out the RTM analysis. D.C. wrote the bulk of the manuscript, with major input from R.W. and T.L.A. R.W. and T.L.A. provided project oversight.

Additional information

The authors declare no competing financial interests. Supplementary Information accompanies this paper on www.nature.com/naturegeoscience. Reprints and permissions information is available online at http://npg.nature.com/reprintsandpermissions. Correspondence and requests for materials should be addressed to D.C.